SrCe$_{0.9}$Sm$_{0.1}$O$_{3-\alpha}$ Compounded with NaCl-KCl as a Composite Electrolyte for Intermediate Temperature Fuel Cell

Ruijuan Shi [1], Wei Chen [2], Wenli Hu [2], Junlong Liu [1,*] and Hongtao Wang [1,*] iD

[1] School of Chemical and Material Engineering, Fuyang Normal College, Fuyang 236037, China; rjshi@fync.edu.cn

[2] Department of science and health, Fuyang Preschool Education College, Fuyang 236015, China; chenwei20062002@163.com (W.C.); huwenli20062002@163.com (W.H.)

*   Correspondence: jlliu@fync.edu.cn (J.L.); hongtaoking3@163.com (H.W.); Tel.: +86-558-2596249 (H.W.); Fax: +86-558-2596703 (H.W.)

check for updates

Abstract: SrCeO$_3$ and SrCe$_{0.9}$Sm$_{0.1}$O$_{3-\alpha}$ were synthesized using a high-temperature solid-state reaction method using Sm$_2$O$_3$, SrCO$_3$, CeO$_2$ as precursors, then the SrCe$_{0.9}$Sm$_{0.1}$O$_{3-\alpha}$-NaCl-KCl composite electrolyte was fabricated by compounding SrCe$_{0.9}$Sm$_{0.1}$O$_{3-\alpha}$ with NaCl-KCl and sintering it at a lower temperature (750 °C) than that of a single SrCeO$_3$ material (1540 °C). The phase and microstructure of the samples were characterized by X-ray diffraction (XRD) and scanning electron microscopy (SEM). The conductivities of the samples were measured in dry nitrogen atmosphere using electrochemical analyzer. The conductivities of the SrCeO$_3$, SrCe$_{0.9}$Sm$_{0.1}$O$_{3-\alpha}$ and SrCe$_{0.9}$Sm$_{0.1}$O$_{3-\alpha}$-NaCl-KCl at 700 °C were 2.09 × 10^{-5} S·cm^{-1}, 1.82 × 10^{-3} S·cm^{-1} and 1.43 × 10^{-1} S·cm^{-1} respectively. The conductivities of SrCe$_{0.9}$Sm$_{0.1}$O$_{3-\alpha}$-NaCl-KCl composite electrolyte are four orders of magnitude higher than those of SrCeO$_3$ and two orders of magnitude higher than those of SrCe$_{0.9}$Sm$_{0.1}$O$_{3-\alpha}$. The result of logσ ~log$p$O$_2$ plot indicates that SrCe$_{0.9}$Sm$_{0.1}$O$_{3-\alpha}$-NaCl-KCl is almost a pure ionic conductor. The electrolyte resistance and the polarization resistance of the H$_2$/O$_2$ fuel cell based on SrCe$_{0.9}$Sm$_{0.1}$O$_{3-\alpha}$-NaCl-KCl composite electrolyte under open-circuit condition were 1.0 Ω·cm^2 and 0.2 Ω·cm^2 respectively. Further, the obtained maximum power density at 700 °C was 182 mW·cm^{-2}.

Keywords: defects; composite; electrolytes; hydrogen; fuel cell; conductivity

1. Introduction

Fuel cells have become one of the hot spots in the fields of new energy and environment protection. This is mainly because they have many advantages like high energy conversion efficiency, quiet operation, low cost and low pollution emission [1–11]. Cathode, anode and solid electrolyte are the vital components of the solid oxide fuel cell (SOFC). The key factor to design a high performance SOFC is the electrolyte. At high temperature, the perovskite-type solid electrolytes based on SrCeO$_3$ exhibits predominant proton conduction under a hydrogen-containing atmosphere. They also have various applications in hydrogen sensor, fuel cell and membrane reactors, etc. Furthermore, partial substitution of the Ce^{4+} by a trivalent rare earth element, such as Eu^{3+}, Y^{3+}, Yb^{3+} and Lu^{3+}, plays an important role in the improvement of the protonic conductivity of SrCeO$_3$ when compared to pure SrCeO$_3$ which exhibits low electronic conductivity [12–18]. Zhang et al. reported Yb doped SrCeO$_3$ powders that were prepared using a low temperature gel combustion method and later studied the effect of ratio of citric acid to metals cations, oxidizer and calcination temperature on the properties of the SrCe$_{0.9}$Yb$_{0.1}$O$_{3-\ddot{o}}$ powders [14]. To investigate the effect of temperature on the total conductivity

and hydrogen fluxes for europium-doped strontium cerate, Shrivastava et al. presented a numerical method to the defect chemical equations to model defect population in $SrCe_{0.95}Eu_{0.05}O_{3-\alpha}$ under hydrogen atmosphere [19]. However, research reveals that there are still challenges because the conductivity of trivalent cations-doped $SrCeO_3$ is not high enough to meet the commercial application of solid oxide fuel cells.

In recent years, composite electrolytes based on doped ceria and alkaline carbonates or halides have been fabricated and exhibited enhanced ionic conductivities, as well as considerable cell power outputs compared to doped ceria [20–26]. Fu et al. suggested that the enhancement of ionic conductivity of gadolinium-doped ceria (GDC)-LiCl-SrCl$_2$ composite electrolyte may be related to the interfaces between GDC and LiCl-SrCl$_2$, which greatly facilitates the increase in the oxygen transfer routes [24,25].

Doped ceria electrolytes are conventional oxide ion conductors. However, there are only a few reports by Huang's group and our group based on composite electrolytes of perovskite-type protonic conductors, such as $BaCeO_3$ and $SrCeO_3$ using inorganic salt for intermediate temperature fuel cell [27–30]. In addition, perovskite-type solid oxide-inorganic salts composite electrolytes have not been developed and investigated thoroughly.

In this work, $SrCeO_3$ and $SrCe_{0.9}Sm_{0.1}O_{3-\alpha}$ were synthesized by a high-temperature solid-state reaction method. The $SrCe_{0.9}Sm_{0.1}O_{3-\alpha}$-NaCl-KCl composite electrolyte was fabricated by compounding $SrCe_{0.9}Sm_{0.1}O_{3-\alpha}$ with NaCl-KCl and sintering at lower temperature (750 °C). The phase and microstructure of the samples were characterized by X-ray diffraction (XRD) and scanning electron microscopy (SEM). The H_2/O_2 fuel cells were also fabricated and conductivities of the samples were measured using electrochemical analyzer in dry nitrogen atmosphere in an operating temperature range of 500–700 °C. The differences between previous studies are compared and addressed.

2. Experimental Section

$SrCeO_3$(SC) and $SrCe_{0.9}Sm_{0.1}O_{3-\alpha}$(SCS) were firstly synthesized using solid-state reaction method. Stoichiometric amounts of raw materials, i.e., Sm_2O_3, $SrCO_3$ and CeO_2 were mixed together and ball milled thoroughly in the presence of anhydrous ethanol. The powdered mixtures were then calcined at 1300 °C for 5 h in air. After they cooled down to room temperature, the resulting powdered samples were finely ground and pelleted. Finally, the pellets were sintered at 1540 °C for 5 h to obtain SC and SCS.

Sodium chloride and potassium chloride were mixed together at a molar ratio of 1:1. Then they were ground thoroughly and placed in a ceramic crucible. After they were heat-treated two times at 700 °C, NaCl-KCl binary molten salt was achieved, which was then mixed with $SrCe_{0.9}Sm_{0.1}O_{3-\alpha}$ powders. The amount of NaCl-KCl molten salts was 20 wt % in the powdered mixture. The mixture was finely grounded and pelleted in a disk which was 18 mm in diameter and 2–3 mm in thickness. The pellet was subsequently calcined at 750 °C for 2 h to obtain $SrCe_{0.9}Sm_{0.1}O_{3-\alpha}$-NaCl-KCl composite electrolyte which were labeled as SCS-NK.

X-ray diffractometry (XRD, X'pert Pro MPD, Holland's company, Amsterdam, the Netherlands) with Cu-kα radiation was carried out to do the structure and phase analysis of SC, SCS and SCS-NK samples and scanning electron microscopy (SEM, S-4700, Hitachi, Tokyo, Japan) was performed to obtain the surface and cross-sectional morphologies of the three pellet samples. The chemical physics changes and phase formation temperature of the $SrCe_{0.9}Sm_{0.1}O_{3-\alpha}$(SCS), $SrCe_{0.9}Sm_{0.1}O_{3-\alpha}$-NaCl-KCl (SCS-NK) and NaCl-KCl powder in the temperature range between room temperature to 800 °C at a heating rate of 15 °C·min^{-1} under nitrogen atmosphere were determined by thermogravimetry analysis and differential scanning calorimetry (TGA-DSC) (TGA-DSC, Universal V 3.7A, TA Instruments, New Castle, DE, USA), respectively.

The electrical conductivity of SC, SCS and SCS-NK pellets (thickness = 1.0–1.1 mm) were measured by means of AC impedance spectroscopy in a three-electrode system over the frequency range from 0.1 Hz to 1 MHz at 500–700 °C in dry nitrogen atmosphere using an electrochemical analyzer (CHI660E,

Chen Hua company, Shanghai, China), the AC amplitude was 20 mV. The conductivity can be calculated from: $\sigma = \frac{L}{R \cdot S}$, where σ is conductivity, L is thickness, R is resistance and S is surface area of electrolyte pellet. The effect of different operating atmospheres and pressures on the electrical conductivity of SCS-NK was also examined. Oxygen's partial pressure was controlled using mixtures of O_2, N_2 and H_2, the partial pressure was also monitored in situ by an oxygen sensor placed in the experimental chamber(Melexis company, Brussels, Belgium) [26–30]. An oxygen concentration cell with platinum electrodes was developed to measure the electromotive force of SCS electrolyte membrane from 500 to 700 °C. A single cell using SCS-NK as an electrolyte membrane was performed in the presence of pure hydrogen acting as the fuel and oxygen as the oxidant. The fuel cell was tested using the linear scanning of current and voltage method within the CHI660E electrochemical analyzer [31–34]. Silver paste (areas = 0.5 cm^2) covered on each side of the electrolyte membrane, they acted as the current collector and porous platinum was used as electrodes. The power density and open circuit voltage were recorded at 700 °C.

3. Results and Discussion

The powder XRD patterns of $SrCeO_3$ (SC), $SrCe_{0.9}Sm_{0.1}O_{3-\alpha}$ (SCS) and $SrCe_{0.9}Sm_{0.1}O_{3-\alpha}$-NaCl-KCl (SCS-NK) are presented in Figure 1. It can be seen that all of three samples having the same main diffraction peaks at 20.75° (110), 29.48° (112), 42.18° (220) and 61.13° (224), this result is consistent with the standard data (JCPDS 082-2370) for the orthorhombic perovskite phase of $SrCeO_3$. It was noted that some additional peaks related to NaCl and KCl salt phase appear in the SCS-NK composite, which reveals that NaCl-KCl salt in the form of crystalline was coexisting with $SrCe_{0.9}Sm_{0.1}O_{3-\alpha}$ and no reaction occurred between $SrCe_{0.9}Sm_{0.1}O_{3-\alpha}$ and NaCl-KCl salt during the process of heat treatment [30].
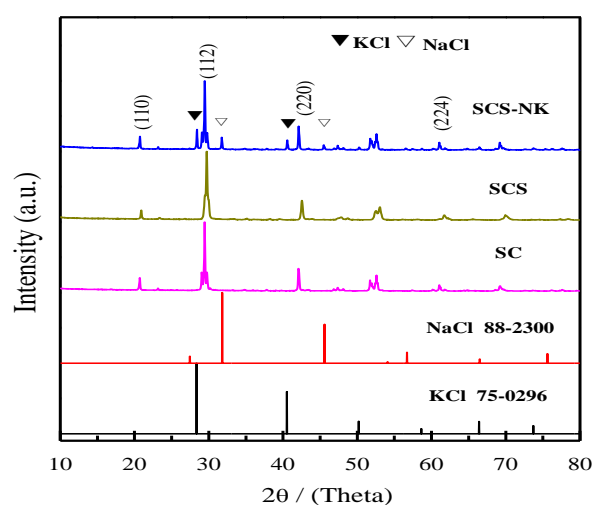
Figure 1. XRD patterns of $SrCeO_3$(SC), $SrCe_{0.9}Sm_{0.1}O_{3-\alpha}$(SCS) and $SrCe_{0.9}Sm_{0.1}O_{3-\alpha}$-NaCl-KCl (SCS-NK) powder.

Figure 2 shows surface (a,c,e) and cross-sectional (b,d,f) SEM images of SC, SCS and SCS-NK pellets. From Figure 2a,b, it can be observed that there are some closed pores on the surface and cross-sectional of SC, but this does not affect the electrical performance test. From Figure 2c,d, it can be seen that the SCS pellet shows more denser powder agglomeration than that of SC, However, a few closed pores still exists. From Figure 2e,f, it is obvious that the low-melting NaCl-KCl salt are closely connected to the surface of SCS powder and the SCS-NK composite electrolyte pellet was fully densified after calcining at 750 °C for 2 h, also there were no pores present [28,29]. This result is like the observation of the ceria-carbonates composite electrolytes in the study by Shawuti [20]. The SCS and NK have been indicated by arrows in Figure 2e.
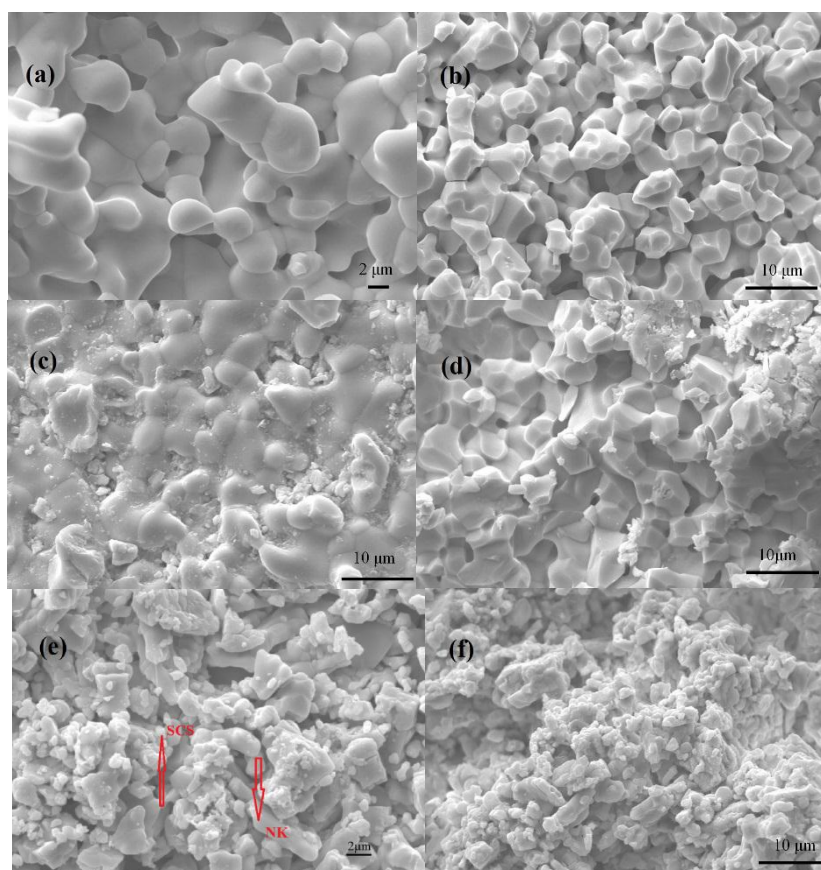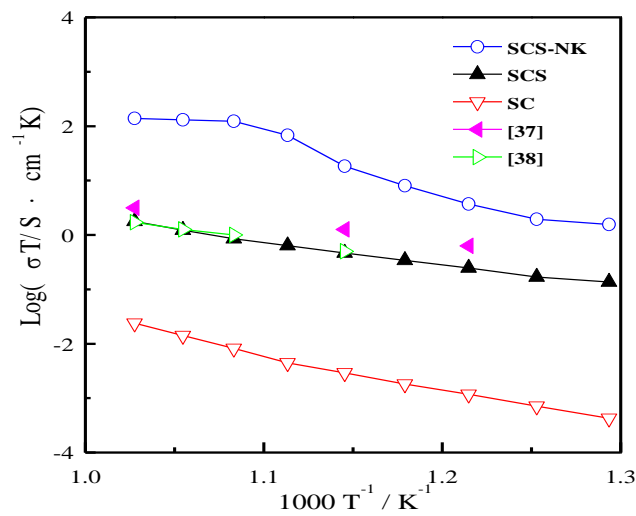
Figure 2. Surface (**a**,**c**,**e**) and cross-sectional (**b**,**d**,**f**) SEM images of $SrCeO_3$(SC), $SrCe_{0.9}Sm_{0.1}O_{3-\alpha}$(SCS) and $SrCe_{0.9}Sm_{0.1}O_{3-\alpha}$-NaCl-KCl (SCS-NK) pellets.

Figure 3 shows the thermogravimetry analysis (TGA) and differential scanning calorimetry (DSC) curves of the $SrCe_{0.9}Sm_{0.1}O_{3-\alpha}$(SCS), $SrCe_{0.9}Sm_{0.1}O_{3-\alpha}$-NaCl-KCl (SCS-NK) and NaCl-KCl powder in the temperature range between room temperature to 800 °C at a heating rate of 15 °C·min^{-1} under nitrogen atmosphere, respectively. In Figure 3a, it is obvious that SCS has almost no weight loss in the whole test temperature range, while the TGA curves of the SCS-NK and NaCl-KCl show weight loss at ca. 720 °C and 670 °C, correspondingly. It can also be speculated that the stability of SCS-NK composite will decrease with the rise in temperature. The DSC curve of NaCl-KCl system has a vertical downward, strong endothermic peak at 655 °C from Figure 3b which is attributed to the melting process of inorganic salt. For the SCS-NK, the endothermic peak at 638 °C corresponds to the melting process changing from crystal to non-crystal in the composite [35,36].

The variation in conductivities of SC, SCS and SCS-NK as a function of temperature in dry nitrogen atmosphere at 500–700 °C is depicted in Figure 4. It is evident that the conductivities were increased with the rise in temperature. SCS showed higher conductivity in comparison to SC and the highest conductivity was shown by SCS-NK composite electrolyte. The conductivities were 5.13×10^{-7} S·cm^{-1}, 1.75×10^{-4} S·cm^{-1} and 1.39×10^{-3} S·cm^{-1} at 500 °C and 2.09×10^{-5} S·cm^{-1}, 1.82×10^{-3} S·cm^{-1} and 1.43×10^{-1} S·cm^{-1} at 700 °C for SC, SCS and SCS-NK, respectively. The conductivities of SCS obtained in this work were compared with the literature data of some $SrCeO_3$ based electrolytes sintered at high temperatures [37,38]. As shown in Figure 4, the conductivities of SCS were comparable to values of $Sr_{0.95}K_{0.05}Ce_{0.95}Y_{0.05}O_3$ [37] and $SrCe_{0.9}Eu_{0.1}O_{3-\alpha}$ [38] under the same condition. It can be attributed to the high temperature solid state reaction method which could result in a dense electrolyte after calcination at 1300 °C and 1540 °C for 5 h, this can be confirmed by the SEM images of Figure 2c,d.
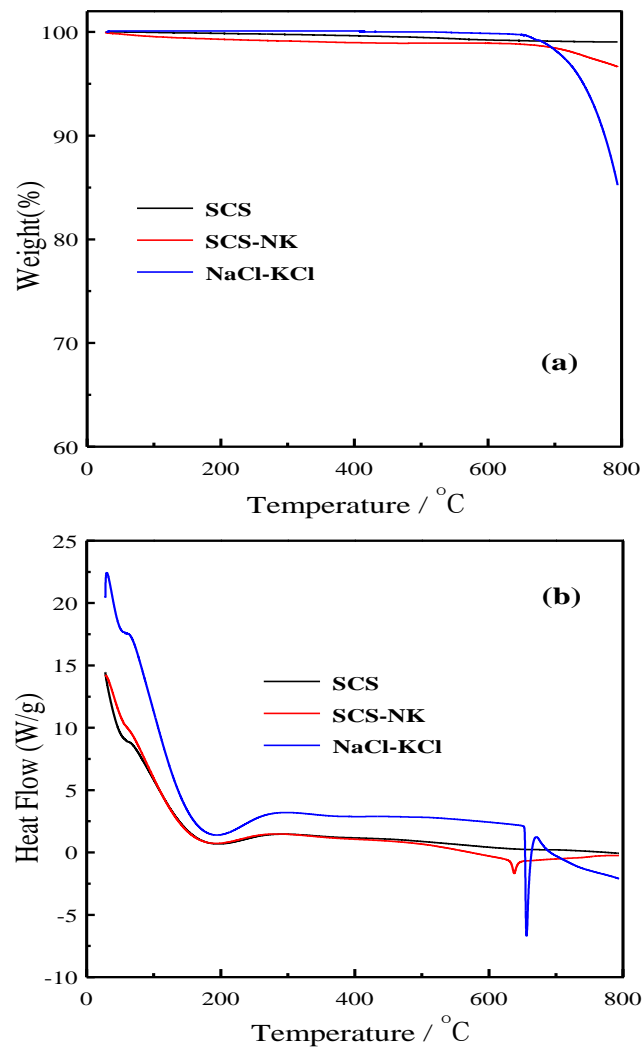
Figure 3. (**a**) TGA, (**b**) DSC curves of the $SrCe_{0.9}Sm_{0.1}O_{3-\alpha}$(SCS), $SrCe_{0.9}Sm_{0.1}O_{3-\alpha}$-NaCl-KCl (SCS-NK) and NaCl-KCl powder in nitrogen up to 800 °C.


Figure 4. Temperature dependence of the conductivities of $SrCeO_3$(SC), $SrCe_{0.9}Sm_{0.1}O_{3-\alpha}$(SCS) and $SrCe_{0.9}Sm_{0.1}O_{3-\alpha}$-NaCl-KCl (SCS-NK) in dry nitrogen atmosphere at 500–700 °C.

In our previous reports [26,30], SrCeO$_3$-based electrolytes were mixed conductors of oxygen ion and electron hole under dry nitrogen atmosphere, whereas here they were mixed conductors of proton, oxygen ion and electron hole under wet nitrogen atmosphere. As we know, protons and oxide ion vacancies are the predominated defects under wet and dry conditions, respectively. In addition, the oxygen-ion diffusion in the conductors need high temperature, whereas protons are the smallest ions and the mobility of protons is much greater compared to that of other ions. Therefore, the conductivity of SrCeO$_3$-based electrolytes is found to be higher in the wet nitrogen atmosphere when compared to dry nitrogen atmosphere.

It is clear that the ionic conductivities in SCS-NK composite electrolyte are four and two orders of magnitude higher than those of SC and SCS at 700 °C, respectively [13,15,16,28,29]. It can be concluded that the NaCl-KCl molten salt that was coated on the surface of SrCe$_{0.9}$Sm$_{0.1}$O$_{3-\alpha}$ and distributed along the grain boundaries, greatly increased the fast ion transfer routes and is beneficial for long distance transport of ions [23,29].

An oxygen concentration cell using SCS as electrolyte membrane was investigated at operating temperatures between 500 and 700 °C. As shown in Figure 5, the observed electromotive force (EMF$_{obs}$) values of the oxygen concentration cell were largely lower than the calculated electromotive force (EMF$_{cal}$) values. The formula to calculate the electromotive force is the same as that described previously [30]. The results show that SCS electrolyte is not a pure ionic conductor, but a mixed conductor of oxide-ion and hole [12,39]. Transport numbers of oxygen ions in SCS electrolytes were 0.34–0.35 which were calculated from the EMF$_{obs}$/EMF$_{cal}$.
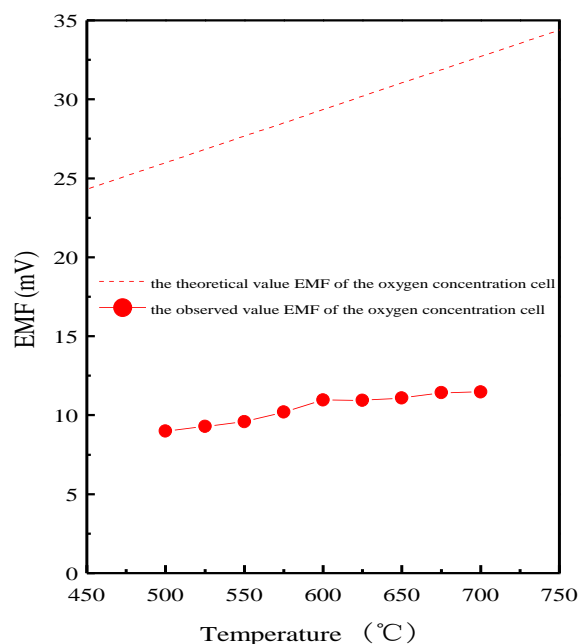

Figure 5. The electromotive force values of the oxygen concentration cell using SrCe$_{0.9}$Sm$_{0.1}$O$_{3-\alpha}$(SCS) as electrolyte in the temperature range from 500 to 700 °C.

Figure 6 shows the conductivity of the SCS-NK composite measured at 700 °C as a function of oxygen partial pressure (*p*O$_2$). As seen in Figure 6, the logσ values do not show any changes over oxygen's partial pressure range of $10^{-17} \sim 10^{-3}$ atm, which suggests that SCS-NK composite electrolyte is virtually a pure ionic conductor. However, there were some minor deviations from linearity in conductivity in oxygen's partial pressure ranging from 10^{-19} to 10^{-17} atm and from 10^{-3} to 10^0 atm, which reveals that SCS-NK composite electrolyte exhibits mixed conductivity and mainly ionic conducting properties over the oxygen partial pressure range [26].
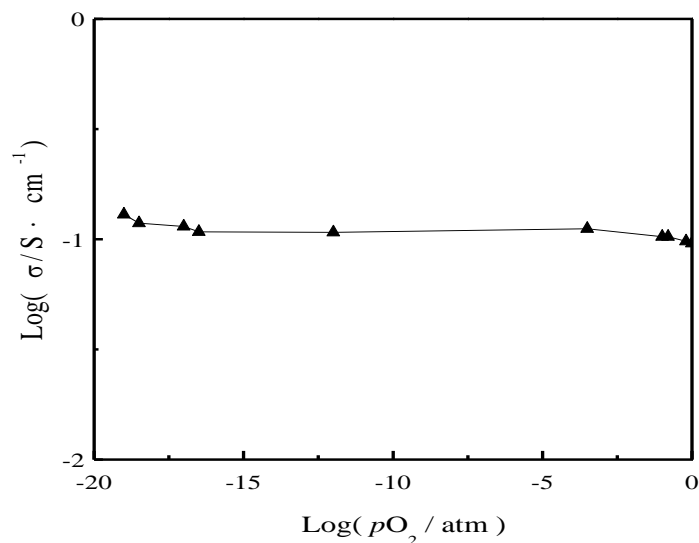
Figure 6. Plot of the conductivity of $SrCe_{0.9}Sm_{0.1}O_{3-\alpha}$-NaCl-KCl (SCS-NK) as a function of pO_2 at 700 °C.

The impedance spectra of SCS and SCS-NK under open-circuit condition at 700 °C are illustrated in Figure 7. The electrolyte resistance values were calculated by the difference in the semicircle diameter between high frequency (HF) and medium frequency (MF), and the polarization resistances values were obtained by the difference in the semicircle diameter between medium frequency (MF) and low frequency (LF). It can be seen that the electrolyte resistance and the polarization resistance for SCS were 3.2 $\Omega\cdot cm^2$ and 1.8 $\Omega\cdot cm^2$, respectively. The electrolyte resistance and the polarization resistance for SCS-NK composite electrolyte were 1.0 $\Omega\cdot cm^2$ and 0.2 $\Omega\cdot cm^2$, respectively [20,21,28,40]. The results indicated that NaCl-KCl molten salt in SCS-NK composite electrolyte, not only provides additional transport routes, but also increases the mobility of the carrier ions, which in turn leads to the decrease in activation energy, thus resulting in a higher electrical performance [40,41].
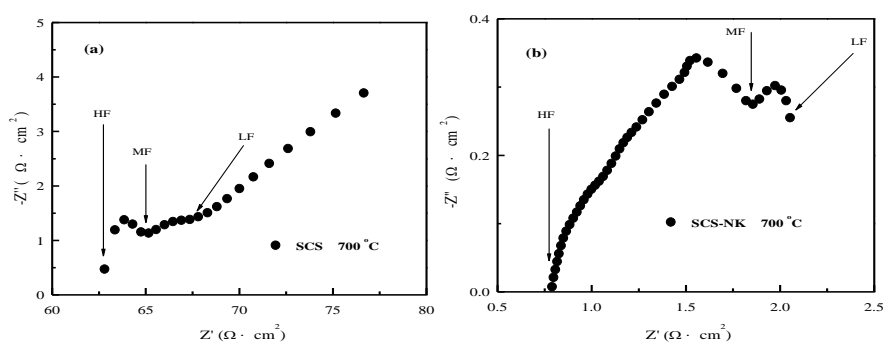
Figure 7. The impedance spectra of the single cells under open-circuit condition at 700 °C. (**a**) $SrCe_{0.9}Sm_{0.1}O_{3-\alpha}$(SCS) and (**b**) $SrCe_{0.9}Sm_{0.1}O_{3-\alpha}$-NaCl-KCl (SCS-NK).

The *I-V-P* curves of the single cells using SCS and SCS-NK as electrolyte membrane at 700 °C by using pure hydrogen as fuel and oxygen as oxidant is shown in Figure 8. The open circuit voltages of the single cells using SCS and SCS-NK as electrolyte were close to the theoretical values, which illustrated that the SCS electrolyte membrane was dense enough after sintered at 1540 °C for 5 h and was the same as the results of Figure 2c,d, on the other hand, it also revealed that $SrCe_{0.9}Sm_{0.1}O_{3-\alpha}$ is fully covered by and closely connected to NaCl-KCl salt to make the SCS-NK composite electrolyte pellet fully dense and facilitate charge carrier transportation. The maximum power density for the single cell using SCS-NK as electrolyte membrane was 182 mW·cm^{-2}, which is more than 47

times higher than that of SCS (3.8 mW·cm^{-2}). Fu et al. reported that the gadolinium-doped ceria (GDC)-LiCl-SrCl$_2$ composite electrolyte shows a maximum power density as high as 260 mW·cm^{-2} at 550 °C which is much higher than that of GDC [24,25].In previous studies by our group, we have demonstrated that the hydrogen–oxygen fuel cells using SrCe$_{0.9}$Gd$_{0.1}$O$_{3-\alpha}$-NaCl-KCl and SrCe$_{0.85}$Er$_{0.15}$O$_{3-\alpha}$-NaCl-KCl composite as electrolytes generates the maximum power densities of 215 mW·cm^{-2} and 304 mW·cm^{-2} at 700 °C, respectively [28,29]. From the results of Figures 4 and 8, we found that the ionic conductivity of SrCe$_{0.9}$Sm$_{0.1}$O$_{3-\alpha}$ was significantly improved when doped with Sm ions and the discharge performance of the SCS-NK composite electrolyte were superior to that of SrCe$_{0.9}$Sm$_{0.1}$O$_{3-\alpha}$ under the same test condition when further combined with NaCl-KCl salt. Such performance may be attributed to the higher ionic conduction of the composite electrolyte, which has been discussed above. However, the durability of the electrolytes have not been tested and will be done as future work.
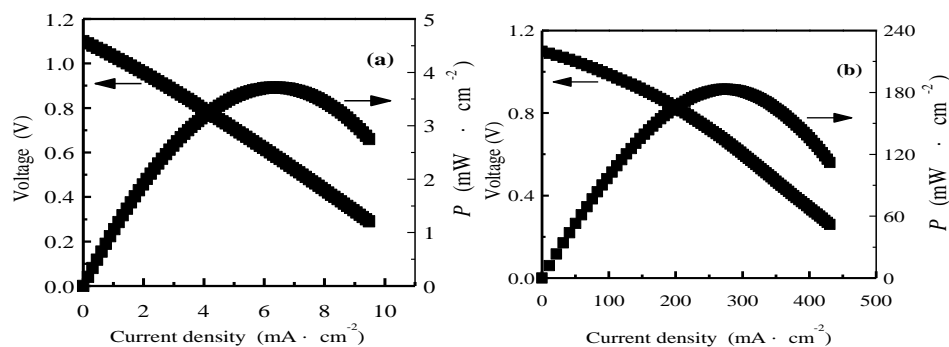
Figure 8. *I-V-P* curves of the single cell with SrCe$_{0.9}$Sm$_{0.1}$O$_{3-\alpha}$(SCS) (**a**) and SrCe$_{0.9}$Sm$_{0.1}$O$_{3-\alpha}$-NaCl-KCl (SCS-NK) (**b**) electrolyte at 700 °C.

4. Conclusions

In summary, the SrCe$_{0.9}$Sm$_{0.1}$O$_{3-\alpha}$-NaCl-KCl composite electrolyte was fabricated by compounding SrCe$_{0.9}$Sm$_{0.1}$O$_{3-\alpha}$ with NaCl-KCl and sintering at much lower temperature (750 °C) than that of single SrCeO$_3$ materials (1540 °C). The conductivity of SrCe$_{0.9}$Sm$_{0.1}$O$_{3-\alpha}$-NaCl-KCl composite electrolyte was 1.43×10^{-1} S·cm^{-1} which is four orders of magnitude higher than that of SrCeO$_3$ and two orders of magnitude higher than that of SrCe$_{0.9}$Sm$_{0.1}$O$_{3-\alpha}$ in dry nitrogen atmosphere at 700 °C. This can be because NaCl-KCl molten salt was distributed along the grain boundaries of SrCe$_{0.9}$Sm$_{0.1}$O$_{3-\alpha}$ which greatly increased the fast ion transfer routes and is beneficial for long distance transport of ions. The electrolyte resistance and the polarization resistance for SrCe$_{0.9}$Sm$_{0.1}$O$_{3-\alpha}$-NaCl-KCl composite electrolyte were 1.0 Ω·cm^2 and 0.2 Ω·cm^2 under open-circuit condition, respectively, and the obtained maximum power density was 182 mW·cm^{-2} at 700 °C, which is much higher than that of SrCe$_{0.9}$Sm$_{0.1}$O$_{3-\alpha}$ (3.8 mW·cm^{-2}).

References

1. Li, J.; Zhang, H.; Gao, M.; Li, Q.; Bian, W.; Tao, T.; Zhang, H. High-temperature wettability and interactions between Y-containing Ni-based alloys and various oxide ceramics. *Materials* **2018**, *11*, 749. [CrossRef] [PubMed]

2. Sadeghifar, H. In-plane and through-plane electrical conductivities and contact resistances of a Mercedes-Benz catalyst-coated membrane, gas diffusion and micro-porous layers and a Ballard graphite bipolar plate: Impact of humidity, compressive load and polytetrafluoroethylene. *Energy Convers. Manag.* **2017**, *154*, 191–202.

3. Kondoh, J. Origin of the hump on the left shoulder of the X-ray diffraction peaks observed in Y_2O_3-fully and partially stabilized ZrO_2. *J. Alloys Compd.* **2004**, *375*, 270–282. [CrossRef]

4. Sadeghifar, H.; Bahrami, M.; Djilali, N. A statistically-based thermal conductivity model for fuel cell Gas Diffusion Layers. *J. Power Sources* **2013**, *233*, 369–379. [CrossRef]

5. Xia, C.; Qiao, Z.; Feng, C.; Kim, J.; Wang, B.; Zhu, B. Study on zinc oxide-based electrolytes in low-temperature solid oxide fuel cells. *Materials* **2018**, *11*, 40. [CrossRef] [PubMed]

6. Sadeghifar, H.; Djilali, N.; Bahrami, M. Effect of Polytetrafluoroethylene (PTFE) and micro porous layer (MPL) on thermal conductivity of fuel cell gas diffusion layers: Modeling and experiments. *J. Power Sources* **2014**, *248*, 632–641. [CrossRef]

7. Sadeghifar, H.; Djilali, N.; Bahrami, M. A new model for thermal contact resistance between fuel cell gas diffusion layers and bipolar plates. *J. Power Sources* **2014**, *266*, 51–59. [CrossRef]

8. Ueno, T.; Hirata, Y.; Shimonosono, T. Analysis of compressive deformation behavior of wet powder compacts of nanometer-sized yttria-stabilized zirconia particles. *Ceram. Int.* **2016**, *42*, 1926–1932. [CrossRef]

9. Bernuy-Lopez, C.; Rioja-Monllor, L.; Nakamura, T.; Ricote, S.; O'Hayre, R.; Amezawa, K.; Einarsrud, M.; Grande, T. Effect of cation ordering on the performance and chemical stability of layered double perovskite cathodes. *Materials* **2018**, *11*, 196. [CrossRef] [PubMed]

10. Sadeghifar, H.; Djilali, N.; Bahrami, M. Thermal conductivity of a graphite bipolar plate (BPP) and its thermal contact resistance with fuel cell gas diffusion layers: Effect of compression, PTFE, micro porous layer (MPL), BPP out-of-flatness and cyclic load. *J. Power Sources* **2015**, *273*, 96–104. [CrossRef]

11. Dankeaw, A.; Poungchan, G.; Panapoy, M.; Ksapabutr, B. In-situ one-step method for fabricating three-dimensional grass-like carbon-doped ZrO_2 films for room temperature alcohol and acetone sensors. *Sensor. Actuators B Chem.* **2017**, *242*, 202–214. [CrossRef]

12. Sammes, N.; Phillips, R.; Smirnova, A. Proton conductivity in stoichiometric and sub-stoichiometric yittrium doped $SrCeO_3$ ceramic electrolytes. *J. Power Sources* **2004**, *134*, 153–159. [CrossRef]

13. Okuyama, Y.; Isa, K.; Lee, Y.S.; Sakai, T.; Matsumoto, H. Incorporation and conduction of proton in $SrCe_{0.9-x}Zr_xY_{0.1}O_{3-\delta}$. *Solid State Ion.* **2015**, *275*, 35–38. [CrossRef]

14. Zhang, C.; Li, S.; Liu, X.; Zhao, X.; He, D.; Qiu, H.; Qiu, Q.; Wang, S.; Jiang, L. Low temperature synthesis of Yb doped $SrCeO_3$ powders by gel combustion process. *Int. J. Hydrogen Energy* **2013**, *38*, 12921–12926. [CrossRef]

15. Xing, W.; Dahl, P.I.; Roaas, L.V.; Fontaine, M.-L.; Larring, Y.; Henriksen, P.P.; Bredesen, R. Hydrogen permeability of $SrCe_{0.7}Zr_{0.25}Ln_{0.05}O_{3-\alpha}$ membranes (Ln = Tm and Yb). *J. Membr. Sci.* **2015**, *473*, 327–332. [CrossRef]

16. Matskevich, N.I.; Wolf, T.; Vyazovkin, I.V.; Adelmann, P. Preparation and stability of a new compound $SrCe_{0.9}Lu_{0.1}O_{2.95}$. *J. Alloys Compd.* **2015**, *628*, 126–129. [CrossRef]

17. Uchida, H.; Maeda, N.; Iwahara, H. Relation between proton and hole conduction in $SrCeO_3$-based solid electrolytes under water-containing atmospheres at high temperatures. *Solid State Ion.* **1983**, *11*, 117–124. [CrossRef]

18. Yuan, W.; Xiao, C.; Li, L. Hydrogen permeation and chemical stability of In-doped $SrCe_{0.95}Tm_{0.05}O_{3-\alpha}$ membranes. *J. Alloys Compd.* **2014**, *616*, 142–147. [CrossRef]

19. Shrivastava, U.N.; Duncan, K.L.; Chung, J.N. ExperimentallyExperimentaly validated numerical modeling of Eu doped $SrCeO_3$ membrane for hydrogen separation. *Int. J. Hydrogen Energy* **2012**, *37*, 15350–15358. [CrossRef]

20. Shawuti, S.; Gulgun, M.A. Solid oxide-molten carbonate nano-composite fuel cells: Particle size effect. *J. Power Sources* **2014**, *267*, 128–135. [CrossRef]

21. Zhu, B.; Li, S.; Mellander, B.E. Theoretical approach on ceria-based two-phase electrolytes for low temperature (300–600 °C) solid oxide fuel cells. *Electrochem. Commun.* **2008**, *10*, 302–305. [CrossRef]

22. Rajesh, S.; Macedo, D.A.; Nascimento, R.M.; Souza, G.L.; Figueiredo, F.M.L.; Marques, F.M.B. One-step synthesis of composite electrolytes of Eu-doped ceria and alkali metal carbonates. *Int. J. Hydrogen Energy* **2013**, *38*, 16539–16545. [CrossRef]

23. Kim, J.-T.; Lee, T.-H.; Park, K.-Y.; Seo, Y.; Kim, K.B.; Song, S.-J.; Park, B.; Park, J.-Y. Electrochemical properties of dual phase neodymium-doped ceria alkali carbonate composite electrolytes in intermediate temperature. *J. Power Sources* **2015**, *275*, 563–572. [CrossRef]

24. Fu, Q.X.; Zhang, W.; Peng, R.R.; Peng, D.K.; Meng, G.Y.; Zhu, B. Doped ceria–chloride composite electrolyte for intermediate temperature ceramic membrane fuel cells. *Mater. Lett.* **2002**, *53*, 186–192. [CrossRef]

25. Fu, Q.X.; Zha, S.W.; Zhang, W.; Peng, D.K.; Meng, G.Y.; Zhu, B. Intermediate temperature fuel cells based on doped Ceria-LiCl-SrCl$_2$ composite electrolyte. *J. Power Sources* **2002**, *104*, 73–78. [CrossRef]

26. Shi, R.; Liu, J.; Wang, H.; Wu, F.; Miao, H. Intermediate temperature fuel cell durability of Eu-doped SrCeO$_3$-SrZrO$_3$ solid solution/NaCl-KCl composite electrolyte. *Ceram. Int.* **2017**, *43*, 16931–16935. [CrossRef]

27. Hei, Y.; Huang, J.; Wang, C.; Mao, Z. Novel doped barium cerateecarbonate composite electrolyte material for low temperature solid oxide fuel cells. *Int. J. Hydrogen Energy* **2014**, *39*, 14328–14333. [CrossRef]

28. Sun, L.; Wang, H.; Sheng, L.; Li, H. Gadolinium doped strontium cerate prepared by citric-nitrate auto-combustion process and intermediate temperature electrical properties of its composite electrolyte. *Int. J. Electrochem. Sci.* **2017**, *12*, 9689–9696. [CrossRef]

29. Guan, Q.; Wang, H.; Miao, H.; Sheng, L.; Li, H. Synthesis and conductivity of strontium cerate doped by erbium oxide and its composite electrolyte for intermediate temperature fuel cell. *Ceram. Int.* **2017**, *43*, 9317–9321. [CrossRef]

30. Shi, R.; Liu, J.; Wang, H.; Wu, F.; Miao, H.; Cui, Y. Low temperature synthesis of SrCe$_{0.9}$Eu$_{0.1}$O$_{3-\alpha}$ by sol-gel method and SrCe$_{0.9}$Eu$_{0.1}$O$_{3-\alpha}$-NaCl-KCl composite electrolyte for intermediate temperature fuel cells. *Int. J. Electrochem. Sci.* **2017**, *12*, 11594–11601. [CrossRef]

31. Sadeghifar, H.; Djilali, N.; Bahrami, M. Counter-intuitive reduction of thermal contact resistance with porosity: A case study of polymer electrolyte membrane fuel cells. *Int. J. Hydrogen Energy* **2014**, *41*, 6833–6841. [CrossRef]

32. Sadeghifar, H. Reconstruction and analysis of fuel cell gas diffusion layers using fiber spacing rather than pore size data: Questioned validity of widely-used porosity-based thermal conductivity models. *J. Power Sources* **2016**, *307*, 673–677. [CrossRef]

33. Sadeghifar, H. An optimized microstructure to minimizing in-plane and through-plane pressure drops of fibrous materials: Counter-intuitive reduction of gas diffusion layer permeability with porosity. *J. Power Sources* **2018**, *385*, 100–113. [CrossRef]

34. Sadeghifar, H. In-plane and through-plane local and average Nusselt numbers in fibrous porous materials with different fiber layer temperatures: Gas diffusion layers for fuel cells. *J. Power Sources* **2016**, *325*, 311–321. [CrossRef]

35. Miranda, M.I.G.; Bica, C.I.D.; Nachtigall, S.M.B.; Rehman, N.; Rosa, S.M.L. Kinetical thermal degradation study of maize straw and soybean hull celluloses by simultaneous DSC–TGA and MDSC techniques. *Thermochim. Acta* **2013**, *565*, 65–71. [CrossRef]

36. Huang, S.; Sheng, J.J. An innovative method to build a comprehensive kinetic model for air injection using TGA/DSC experiments. *Fuel* **2017**, *210*, 98–106. [CrossRef]

37. Liu, C.; Huang, J.-J.; Fu, Y.-P.; Li, C.; Wang, J.-Y.; Lee, S. Effect of potassium substituted for A-site of SrCe$_{0.95}$Y$_{0.05}$O$_3$ on microstructure, conductivity and chemical stability. *Ceram. Int.* **2015**, *41*, 2948–2954. [CrossRef]

38. Tsuji, T.; Nagano, T. Electrical conduction in SrCeO$_3$ doped with Eu$_2$O$_3$. *Solid State Ion.* **2000**, *136–137*, 179–182. [CrossRef]

39. Philips, R.J.; Bonanos, N.; Poulsen, F.W.; Ahlgren, E.O. Structural and electrical characterisation of SrCe$_{1-x}$Y$_x$O$_\xi$. *Solid State Ion.* **1999**, *125*, 389–395. [CrossRef]

40. Jaiswal, N.; Singh, N.K.; Kumar, D.; Parkash, O. Effect of strontium (Sr) doping on the conductivity of ceria. *J. Power Sources* **2012**, *202*, 78–84. [CrossRef]

41. Tanwar, K.; Jaiswal, N.; Sharma, P.; Kumar, D.; Parkash, O. Structural analysis of Ce$_{0.83}$Dy$_{0.14}$Ca$_{0.03}$O$_{1.90}$ (CDC) and enhanced electrical conductivity of its composites with alkali carbonates for LT-SOFCs. *J. Alloys Compd.* **2018**, *741*, 532–541. [CrossRef]